Analysis of Curved Metasurfaces with Spatially-Varying Impedance Distribution

Zvonimir Sipus[1], Dominik Barbaric[2] and Marko Bosiljevac[1]
[1.] Faculty of Electrical Engineering and Computing, University of Zagreb, Croatia
[2.] Ericsson Nikola Tesla d.d. Research and Development Centre, Zagreb, Croatia
e-mail: zvonimir.sipus@fer.hr, dominik.barbaric@ericsson.com, marko.bosiljevac@fer.hr

***Abstract*—Metasurfaces have garnered significant attention in recent years as devices that direct waves, manipulate the polarization of transmitted or reflected waves, or influence spectral properties of those waves. Until now, most of the attention was focused on the development of planar metasurface structures. However, many demanding electromagnetic applications require the implementation of curved structures. In this paper, we propose an analysis approach for curved metasurfaces that are not homogeneous, i.e. metasurfaces that have spatially-varying distribution of surface sheet impedance. The considered formulation also covers metasurfaces that do not encompass the entire canonical curved surface. The results are verified against several experimentally characterized cylindrical metasurface examples.**

***Index Terms*— metasurfaces, curved metasurfaces, spectral domain aproach, sheet impedance, PCB metasurface.**

I. INTRODUCTION

Various electromagnetic periodic surfaces, popularly known as metasurfaces, have numerous new possibilities for manipulating the direction and polarization properties of transmitted electromagnetic waves. Traditionally, resonant elements were used in design of periodic frequency selective surfaces (FSS). However, recent designs use sub-wavelength elements as building blocks, which enabled a wider range of functionality, such as focusing, beam tilting, polarization manipulation, increased bandwidth etc. (see e.g. [1] - [4]).

While previous works mostly focused on planar metasurface structures, we find interest in exploring curved metasurfaces since many applications can have such electromagnetic, aerodynamic or mechanical constraints. However, introduction of curvature significantly complicates analysis and design, since the quasi-infinite periodicity used in planar structures is lost in most cases. Furthermore, the considered structures are very large in terms of wavelength and they contain a lot of small metallic details within each of the metasurface layers (by definition, the unit cell of the metasurface pattern is much smaller than the wavelength). Due to the complexity of solving design problems for large finite structures with numerous small cells, using general electromagnetic solvers would result in very long computation times, and excess memory requirements. With all this in mind, to successfully design curved metasurface structures, one needs to develop specialized efficient numerical analysis algorithms. Analytical and quasi-analytical approaches to the design of curved metasurfaces can be found in [5] - [8].

Some metasurface-based devices, such as cylindrical or spherical cloaks, would require homogeneous distribution of surface impedance. However, many devices require spatially-varying impedance distribution to modulate the amplitude and phase of incoming wave. Often, the considered metasurface is occupying only a part of canonical surface, such as a cylinder or a sphere. We propose an analysis approach for canonical curved structures which is generalized so that it can include a class of metasurface structures with spatially-varying impedance distribution, including such structures that do not span the entire canonical surface. The presented analysis method is based on Green's functions approach and it is demonstrated for a cylindrical case. However, it can easily be generalized for other types of geometries (e.g. spherical, Body-of-Revolution, etc.). The basis of the analysis approach is the method for spatially-uniform metasurfaces, described in [6].

II. ANALYSIS APPROACH

The geometry of the considered cylindrical problem is shown in Fig. 1. Each metasurface layer is modelled by a penetrable sheet impedance boundary condition. Without losing generality, we will assume that the considered metasurface has electric response only. The sheet can then be represented by an admittance tensor $\bar{\bar{Y}}(\phi, z)$. The boundary condition to be satisfied is the following:

$$\bar{\bar{Y}}(\phi, z) \cdot \mathbf{E}(\rho_{\text{meta}}, \phi, z) = \hat{\rho} \times \Delta\mathbf{H}(\rho_{\text{meta}}, \phi, z), \qquad (1)$$

where $\Delta\mathbf{H}$ represents the magnetic field discontinuity between the outer and inner boundary of the metasurface. The cylindrical metasurface can also be placed only at the part of the cylindrical tube. For the rest of the tube we can impose the following boundary condition:

$$\hat{\rho} \times \Delta\mathbf{H}(\rho_{\text{meta}}, \phi, z) = 0. \qquad (2)$$

The two boundary conditions can be merged if the unpopulated part of the cylindrical tube is expressed as a

zero-admittance sheet. Now, the boundary condition for the whole cylindrical interface is given by eq. (1).

The analysis procedure will be introduced in two steps. First, we will analyse a basic one-layer metasurface problem, and in the second step we will generalize the analysis approach to multi-layer multi-metasurface structures.

Basic two-dimensional (2D) formulation

The considered 2D metasurface is non-homogeneous in ϕ-direction and homogeneous in the axial direction. The metasurface is located in free space, and it is excited from the central axis; i.e. the excitation is a constant current line source. These assumptions will be generalized in the next section.

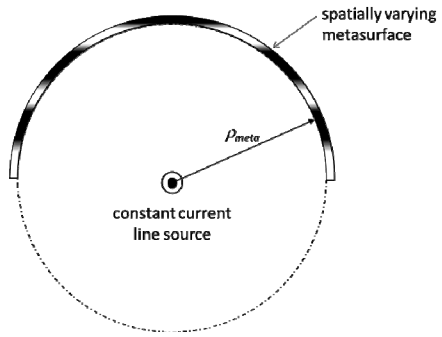

(a)

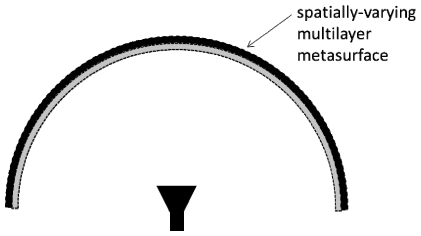

(b)

Fig. 1. Geometry of a curved metasurface structure with spatially-varying value of surface sheet impedance; (a) basic 2D geometry, (b) general multilayer multi-metasurface with an arbitrary feed antenna.

The incident field excited by a constant-current electric line source is:

$$E_z^{\text{inc}}(\rho,\phi) = -\frac{k_0\eta_0}{4} H_0^{(2)}(k\rho)\cdot I_0 \tag{3.a}$$

$$H_\phi^{\text{inc}}(\rho,\phi) = -j\frac{k_0}{4} H_1^{(2)}(k_0\rho)\cdot I_0 . \tag{3.b}$$

Here, I_0 is the amplitude of the line source current. Under these assumptions we can write the field distribution in regions inside and outside the cylinder:

(a) the inner region

$$E_z^{\text{tot}} = E_z^{\text{inc}} + E_z^{\text{scat}}$$

$$E_z^{\text{tot}}(\rho,\phi) = -\frac{k_0\eta_0}{4} H_0^{(2)}(k_0\rho) I_0 + \sum_{m=-\infty}^{\infty} \alpha_m^{(1)} J_m(k_0\rho) e^{-jm\phi} \tag{4.a}$$

$$H_\phi^{\text{tot}} = H_\phi^{\text{inc}} + H_\phi^{\text{scat}}$$

$$H_\phi^{\text{tot}}(\rho,\phi) = -\frac{jk_0}{4} H_1^{(2)}(k_0\rho) I_0 + \left(\frac{-j}{\eta_0}\right) \sum_{m=-\infty}^{\infty} \alpha_m^{(1)} J_m'(k_0\rho) e^{-jm\phi} \tag{4.b}$$

(b) the outer region

$$E_z^{\text{tot}} = E_z^{\text{inc}} + E_z^{\text{scat}}$$

$$E_z^{\text{tot}}(\rho,\phi) = -\frac{k_0\eta_0}{4} H_0^{(2)}(k_0\rho) I_0 + \sum_{m=-\infty}^{\infty} \alpha_m^{(2)} H_m^{(2)}(k_0\rho) e^{-jm\phi} \tag{5.a}$$

$$H_\phi^{\text{tot}} = H_\phi^{\text{inc}} + H_\phi^{\text{scat}}$$

$$H_\phi^{\text{tot}}(\rho,\phi) = -\frac{jk_0}{4} H_1^{(2)}(k_0\rho) I_0 + \left(\frac{-j}{\eta_0}\right) \sum_{m=-\infty}^{\infty} \alpha_m^{(2)} H_0^{(2)\prime}(k_0\rho) e^{-jm\phi} \tag{5.b}$$

Here, $\alpha_m^{(1)}$ and $\alpha_m^{(2)}$ are the amplitudes of spectral-domain scattered field components in the inner and outer region, respectively. Note that the H_z and E_ϕ components are zero for the considered metasurface structure and line source excitation. In other words, we assumed that the metasurface does not excite cross-polar components.

Now, we arrive at the following system of equations:

$$E_z^{\text{scat},(1)}(\rho_{\text{meta}},\phi) = E_z^{\text{scat},(2)}(\rho_{\text{meta}},\phi) \tag{6.a}$$

$$\begin{aligned} Y_{zz}(\phi)\cdot\left[E_z^{\text{inc}}(\rho_{\text{meta}},\phi) + E_z^{\text{scat},(2)}(\rho_{\text{meta}},\phi)\right], \\ = H_z^{\text{scat},(2)}(\rho_{\text{meta}},\phi) - H_z^{\text{scat},(1)}(\rho_{\text{meta}},\phi) \end{aligned} \tag{6.b}$$

or, in more details

$$\alpha_m^{(1)} J_m(k_0\rho_{\text{meta}}) = \alpha_m^{(2)} H_m^{(2)}(k_0\rho_{\text{meta}}) \qquad \forall m\in\mathbb{Z} \tag{7.a}$$

$$\begin{aligned} &Y_{zz}(\phi)\cdot\left[-\frac{k_0\eta_0}{4} H_0^{(2)}(k_0\rho_{\text{meta}}) I_0 + \frac{1}{2\pi}\sum_{m=-\infty}^{\infty} \alpha_m^{(2)} H_m^{(2)}(k_0\rho_{\text{meta}}) e^{-jm\phi}\right] \\ &= \left(\frac{-j}{\eta_0}\right)\left[\frac{1}{2\pi}\sum_{m=-\infty}^{\infty} \alpha_m^{(2)} H_m^{(2)\prime}(k_0\rho_{\text{meta}}) e^{-jm\phi}\right. \\ &\left. -\frac{1}{2\pi}\sum_{m=-\infty}^{\infty} \alpha_m^{(1)} J_m'(k_0\rho_{\text{meta}}) e^{-jm\phi}\right]. \end{aligned} \tag{7.b}$$

Here, indices (1) and (2) denote the inner and outer region, respectively, and $Y_{zz}(\phi)$ is the *zz*-component of sheet admittance tensor $\overline{\overline{Y}}(\phi)$.

Equation (7) is the basis for the proposed analysis method. The unknowns in (7) are spectral-domain coefficients α_m of the averaged scattered tangential E-field component along the metasurface. If we determine the limit in summation as M_{max}, we need to select $2 \cdot M_{max}+1$ observation points to obtain a linear system of $2 \cdot M_{max}+1$ equations with $2 \cdot M_{max}+1$ unknowns:

$$\begin{aligned} & Y_{zz}(\phi_n) \cdot \left[-\frac{k_0 \eta_0}{4} H_0^{(2)}(k_0 \rho_{\text{meta}}) I_0 \right. \\ & \left. + \frac{1}{2\pi} \sum_{m=-M_{\max}}^{M_{\max}} \alpha_m^{(2)} H_m^{(2)}(k_0 \rho_{\text{meta}}) e^{-jm\phi_n} \right] \\ & = \left(\frac{-j}{\eta_0} \right) \left[\frac{1}{2\pi} \sum_{m=-\infty}^{\infty} \alpha_m^{(2)} H_m^{(2)\prime}(k_0 \rho_{\text{meta}}) e^{-jm\phi_n} \right. \\ & \left. - \frac{1}{2\pi} \sum_{m=-\infty}^{\infty} \alpha_m^{(1)} J_m'(k_0 \rho_{\text{meta}}) e^{-jm\phi_n} \right] \\ & n = 1, \ldots, 2M_{\max}+1 \end{aligned} \tag{8}$$

The minimum number for M_{max} is $\lfloor k_0 \rho_{\text{meta}} \rfloor$, where $\lfloor \cdot \rfloor$ denotes the *floor* operator. More accurate results are obtained with $M_{\max} = 2 \cdot \lfloor k_0 \rho_{\text{meta}} \rfloor$. Usually, one observation point is located at the centre of each metasurface cell. However, if the selected M_{max} is large, more than one observation point can be located on each metasurface cell.

General three-dimensional (3D) formulation

This solution procedure can be rewritten using the Green's function approach that is suitable for multilayer structures containing cascaded metasurface sheets. The following modifications are needed:

(a) Introduction of induced surface electric currents to model electric response of metasurfaces, i.e. to model the discontinuity in the tangential magnetic field. We find the current as

$$\mathbf{J}_{av} = \hat{n} \times (\mathbf{H}^+ - \mathbf{H}^-) = \hat{\rho} \times \Delta \mathbf{H}, \tag{9}$$

where $\mathbf{H}^+$ and $\mathbf{H}^-$ are magnetic fields on the outer and the inner boundary of the metasurface, respectively. Thus, the response of several stacked metasurface sheets (including mutual coupling between the sheets) can be modelled.

(b) Implementation of spectral-domain Green's function to include the influence of multilayer dielectric supporting structure. As an example, the G1DMULT algorithm can be used [9], [10].

(c) Implementation of the Fourier transformation in *z*-direction to model the spatial variation of metasurface admittance in axial direction.

(d) Implementation of the Moment Method (MoM) procedure to solve the equation (1). The method is based on approximating the induced surface electric current $\mathbf{J}_{av}$ with a set of basis functions $\mathbf{J}_{av}^i$ having unknown amplitudes α_i:

$$\mathbf{J}_{av}(\rho, \phi) = \left[\sum_{i=1}^{N_{MoM}} \alpha_i \mathbf{J}_{av}^i(\rho_{\text{meta}}^i, \phi) \right] \tag{10}$$

The final system of MoM equations has a form (given for 2D case, as derived from an axially uniform structure):

$$\begin{aligned} & \int_{L_j} \mathbf{J}_{av}^j(\rho_{\text{meta}}^j, \phi) \cdot \left[\overline{\overline{Y}}(\rho_{\text{meta}}^j, \phi) \cdot \left[\mathbf{E}^{\text{inc}}(\rho_{\text{meta}}^j, \phi) \right. \right. \\ & \left. \left. + \frac{1}{2\pi} \sum_{m=-M_{\max}}^{M_{\max}} \sum_{i=1}^{N_{MoM}} \alpha_i \, \tilde{\overline{\overline{G}}}^{EJ}(m, \rho_{\text{meta}}^j \left| \rho_{\text{meta}}^i \right.) \cdot \tilde{\mathbf{J}}_{av}^i(\rho_{\text{meta}}^i, m) e^{-jm\phi} \right] \right] d\phi \\ & = \int_{L_j} \mathbf{J}_{av}^j(\rho_{\text{meta}}^j, \phi) \cdot \left[\sum_{i=1}^{N_{MoM}} \alpha_i \mathbf{J}_{av}^i(\rho_{\text{meta}}^i, \phi) \right] d\phi \qquad j = 1, \ldots, N_{MoM} \end{aligned} \tag{11}$$

III. RESULTS

Let us consider a single-layer cylindrical metasurface printed on a thin substrate (ε_r = 2.55, h = 0.13 mm). The idea behind the design is to shape the omnidirectional incident field, originating from the structure's axis, and to form two main beams at angles ±45°, at the operating frequency of 10 GHz. The metasurface contains 24 inductive cells that are in practice realized using stripes or meander lines. The radius of the cylinder is 6 cm and the width of each cell is 7.854 mm. Only half of the cylinder is covered with the metasurface structure. The variation of surface sheet impedance, and the practical realization is shown in Figure 2. The picture of the built prototype is given in Fig. 3. The prototype was developed using standard PCB technology. The flexibility of used PCB substrate was sufficient to bend the PCB structure into a half-cylinder form with a radius of 6 cm.

For additional verification, the metasurface structure is also simulated using CST Microwave Studio. A comparison between radiated field, calculated using the proposed analysis method, and general electromagnetic solver, is given in Fig. 4. The excitation is an omnidirectional line source (in practice, a monopole antenna was used), and the results show good agreement between the two analysis methods and measurements. Note that the spectral-domain method uses surface sheet impedance approach, while CST Microwave Studio results are calculated by considering the developed

metasurface geometry with all the details, whilst skipping the intermediate calculation of surface sheet impedances. Consequently, the needed computation time is several orders of magnitude larger when using the commercial software package. In this particular case, the CST Microwave Studio needed 2 h 50 min in a dual-threaded solver process to obtain the results, while the newly developed program had finished in a second.

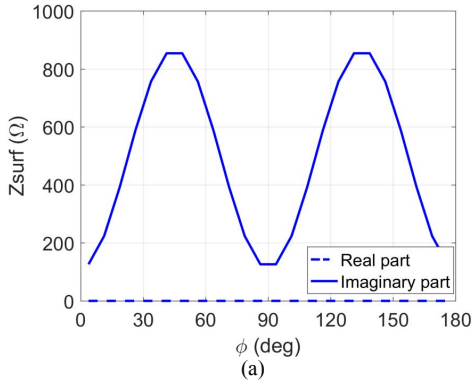

(a)

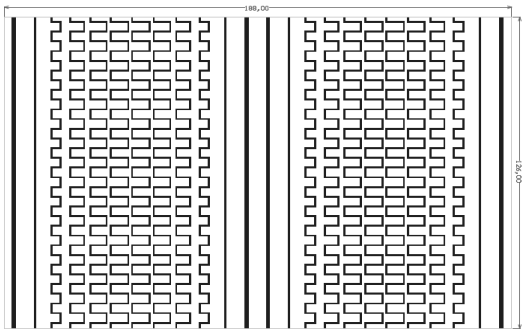

(b)

Fig. 2. (a) Variation of the surface sheet impendance, and (b) PCB layer of a realization featuring meander lines.

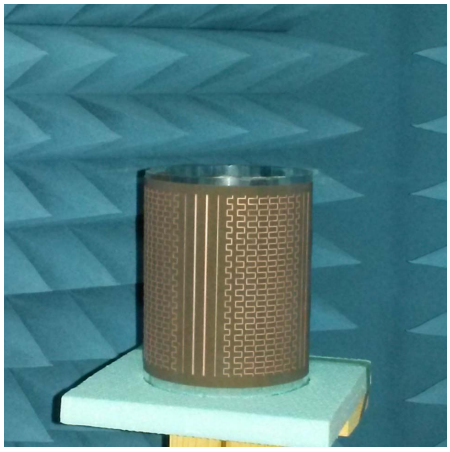

Fig. 3. Realization of a single-layer PCB metasurface.

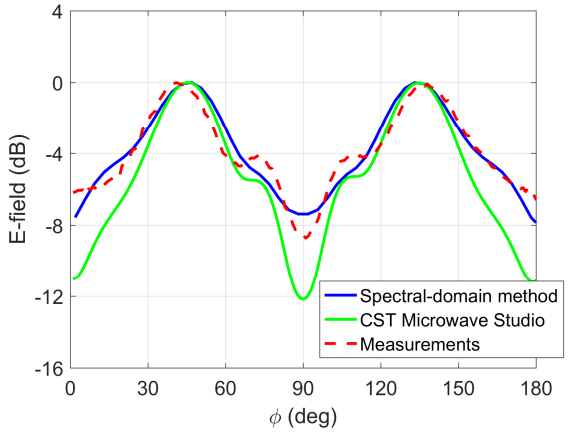

Fig. 4. Electric response of a curved metasurface printed on a thin supporting dielectric structure. Comparison of mesurements and calculations from the developed spectral-domain method and CST Microwave Studio.

From a mechanical point of view, it would be beneficial to mount the metasurface on a solid supporting structure. We used a plexiglass cylinder with an outer radius of 6 cm, thickness of $h = 3.0$ mm, and relative permitivity of $\varepsilon_r = 2.6$. The influence of the supporting structure on radiation properties was investigated. The results are shown in Fig. 5. It can be seen that a thick dielectric support introduces more pronounced resonances in the radiation pattern. These appear due to internal reflections within the plexiglass frame. Furthermore, it can be seen that both analysis methods accurately predict the influence of the supporting structure.

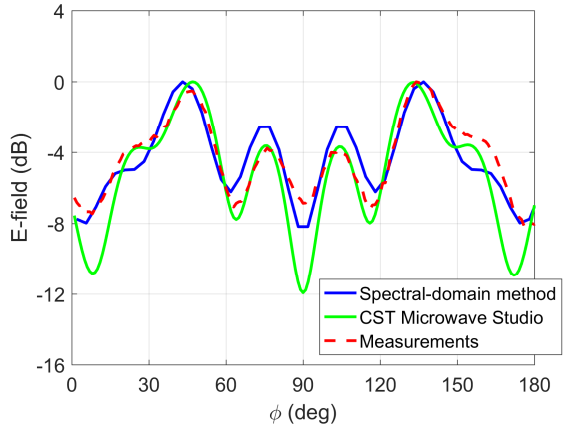

Fig. 5. Electric response of a curved metasurface mounted on a thick supporting dielectric structure. Comparison of mesurements and calculations from the developed spectral-domain method and CST Microwave Studio.

IV. CONCLUSION

The analysis of metasurfaces with non-homogeneous surface impedance was conducted using surface sheet impedance and Green's function approach. The results of the developed method were compared with those achieved by using commercial software, and with measurements, which showed an excellent level of agreement. The developed approach produces considerable time savings, in comparison to using general electromagnetic solvers.

The presented analysis can be easily modified for other types of structures, such as spherical metasurfaces or generalized Body-of-Revolution structures, and therefore represents a valuable tool in the design of novel curved metasurfaces.

ACKNOWLEDGMENT

This work was supported in part by the Air Force Office of Scientific Research, Air Force Material Command, USAF under Award No. FA9550-15-1-0121; by Croatian Science Foundation under the project IP-2018-01-9753; and by Ericsson Nikola Tesla d.d. and University of Zagreb Faculty of Electrical Engineering and Computing under the EWITA project.

REFERENCES

[1] C. Holloway, E. Kuester, J. Gordon, J. O'Hara, J. Booth, and D. Smith, "An overview of the theory and applications of metasurfaces: The twodimensional equivalents of metamaterials," *IEEE Antennas Propag. Mag.*, Vol. 54, no. 2, pp. 10–35, April 2012.

[2] S. Maci, G. Minatti, M. Casaletti, and M. Bosiljevac, "Metasurfing: Addressing waves on impenetrable metasurfaces," *IEEE Antennas Wireless Propag. Lett.,* Vol. 10, pp. 1499–1502, 2011.

[3] C. Pfeiffer and A. Grbic, "Metamaterial Huygens' surfaces: Tailoring wave fronts with reflectionless sheets, " *Phys. Rev. Lett.*, Vol. 110, 2013, Art. ID 197401.

[4] C. Pfeiffer and A. Grbic, "Bianisotropic metasurfaces for optimal polarization control: Analysis and synthesis," *Physical Review Applied*, Vol. 2, Art. ID 044011, October 2014.

[5] P.-Y. Chen, and A. Alu, "Mantle cloaking using thin patterned metasurfaces," *Phys. Rev. B,* Vol. 84, Art. ID 205110, 2011.

[6] Z. Sipus, M. Bosiljevac, A.Grbic, "Modelling Cascaded Cylindrical Metasurfaces Using Sheet Impedances and a Transmission Matrix Formulation," *IET Microwaves Antennas & Propagation*, Vol. 12, No. 7, pp. 1041-1047, 2018.

[7] J. Y. H. Teo, L. J. Wong, C. Molardi, and P. Genevet, "Controlling electromagnetic fields at boundaries of arbitrary geometries. " *Phys. Rev. A*, Vol. 94, Art. ID 023820, 2016.

[8] B. O. Raeker and S. M. Rudolph, "Arbitrary Transformation of Antenna Radiation Using a Cylindrical Impedance Metasurface," *IEEE Antennas Wireless Propag. Lett.,* Vol. 15, pp. 1101-1104, 2016.

[9] Z. Sipus, P.-S. Kildal, R. Leijon, and M. Johansson, "An algorithm for calculating Green's functions for planar, circular cylindrical and spherical multilayer substrates," *Applied Computational Electromagnetics Society Journal*, Vol. 13, pp. 243-254, Nov. 1998.

[10] P.-S. Kildal, Z. Sipus, J. Yang, R. Maaskant, "Useful Physical Images and Algorithms for Vector Dyadic Green's Functions in 3D Spatial, 2D Spectral and 1D Spectral Domains for Solving Multilayer and Multiregion Field Problems," *IEEE Antennas & Propagation Magazine*, Vol. 59, No. 4, pp. 106-116, Aug. 2017.